Polyhedron 27 (2008) 2867–2876

Contents lists available at ScienceDirect

Polyhedron

journal homepage: www.elsevier.com/locate/poly

Synthesis and characterization of thiosemicarbazone derivatives of 2-ethoxy-3-methoxy-benzaldehyde and their rhenium(I) complexes

Ara Núñez-Montenegro, Rosa Carballo, Ezequiel M. Vázquez-López *

Departamento de Química Inorgánica, Facultade de Química, Edificio de Ciencias Experimentais, Universidade de Vigo, E-36310 Vigo, Galicia, Spain

ARTICLE INFO

Article history:
Received 6 April 2008
Accepted 17 June 2008
Available online 26 July 2008

Keywords:
Thiosemicarbazone
Rhenium complexes
Carbonyl complexes
X-ray

ABSTRACT

The ligands (HL^1, HL^2 and HL^3) have been prepared and their reaction with *fac*-$[ReX(CO)_3(CH_3CN)_2]$ (X = Br, Cl) in chloroform gave the adducts $[ReX(CO)_3(HL)]$ (**1a** X = Cl, R = H; **1a′** X = Br, R = H; **1b** X = Cl, R = CH_3; **1b′** X = Br, R = CH_3; **1c** X = Cl, R = Ph; **1c′** X = Br, R = Ph) in good yield. All the compounds have been characterized by elemental analysis, mass spectrometry (FAB), IR and ^{1}H NMR spectroscopic methods, and the structures of the ligands have been elucidated by X-ray diffraction. In the case of HL^1, we have tried the reaction with $[ReX(CO)_5]$ (X = Br, Cl) in toluene and we proved the formation of the adduct also by this way by the isolation of single crystals of **1a′** · ½C_7H_8.

In **1a′**, the rhenium atom is coordinated by the sulfur and the azomethine nitrogen atoms, forming a five-membered chelate ring, as well as three carbonyl carbon and bromine atoms. The resulting coordination polyhedron can be described as a distorted octahedron.

The study of the crystals obtained by slow evaporation of methanol solutions of the adducts **1b** and **1c** showed the formation of dimer structures based on rhenium(I) thiosemicarbazones $[Re_2(L^2)_2(CO)_6]$ (**2b**) and $[Re_2(L^3)_2(CO)_6]$ · 2(CH_3OH) (**2c**) · 2(CH_3OH). The thiosemicarbazonate complexes $[Re_2(L)_2(CO)_6]$ (**2**) were obtained by reaction of the adducts with NaOH in dry methanol.

In **2b** and **2c** · 2(CH_3OH) the dimer structures are established by Re–S–Re bridges, where S is the thiolate sulfur from a N,S-bidentate thiosemicarbazonate ligand. In both structures the rhenium coordination sphere is similar though, they are different in the ligand direction since centrosymmetric dimers are formed in **2c** meanwhile in **2b** are in the same diamond Re_2S_2 face.

1. Introduction

The use of the *fac*-$[M(CO)_3]^+$ (M = ^{99m}Tc and Re) core has been explored widely as diagnostic or radio- and chemotherapeutic agents. For example, Alberto's group has recently shown that $[M(H_2O)_3(CO)_3]^+$ forms complexes with guanine with rate constants of the same order of magnitude as one of the active derivatives of cisplatin $[Pt(NH_3)_2(H_2O)_2]^{2+}$ [1,2]. However, this compound interacts unspecifically with potential coordination sites of human proteins in serum [3]. Therefore, to maintain the availability of the fragment *fac*-$[M(CO)_3]^+$ in relevant concentrations for therapeutic use, the protection of coordination sites is required by ligands that must also be sufficiently labile to be displaced by targeted molecules. In addition, from a therapeutic point of view, the presence of three carbonyl groups reduces molecular weight of the agent and its non-specific uptake could decrease [4].

On the other hand, the studies of Tc(I) tracers agents designed for cardiac perfusion suggested that they must be sufficiently lipophilic for their incorporation and retention in the myocardium [4]. The literature for cardiac perfusion tracers suggest that ether groups can be used to modulate lipophility and physicochemical parameters (molecular weight and volume) that greatly influence cardiac uptake, membrane diffusion, and plasma protein binding. In fact, ether substituents are commonly employed in commercial cardiac perfusion agents such as CARDIOLITE® (BMS) and MYOVIEW® (G.E. Healthcare).

Thiosemicarbazones (TSCs) are very versatile ligands that can coordinate as neutral ligands or in their deprotonated form, so they can have an important variety of coordination modes [5–7]. The inclusion of potential donors groups has been explored to increase ligand denticity or the introduction of organic/metal–organic groups that give the complex molecule different properties. The introduction of 2-pyridincarbaldehyde, 2-acetylpyridine [8], 2,2′-dipyridilcetone [9] and 4-acetylpyridine [10] fragments showed the effects of these donors groups in the thiosemicarbazide chain proximities on the coordination behaviour, or the ferrocenylcarbaldehyde group [11] allowed to study the capacity of the TSCs to communicate the metal and the redox units through the TSC chain.

Furthermore, these types of ligands and their complexes have received considerable attention according to their biological activity. In a recent revision of the pharmacological properties of thio-

* Corresponding author.
E-mail address: ezequiel@uvigo.es (E.M. Vázquez-López).

0277-5387/$ - see front matter © 2008 Elsevier Ltd. All rights reserved.
doi:10.1016/j.poly.2008.06.018

semicarbazone complexes, Quiroga and Navarro have observed the sensible increase in the number of studies of their antibacterial, antiviral, antifungal and antitumour activity [12]. For instance, a report of Cu^{II}, Zn^{II}, Cd^{II} or Hg^{II} complexes with thiosemicarbazone derived from vanillin shows their activity against pathogen fungus belonging to the groups *Alternaria* (sp.), *Paecilomyces* (sp.) and *Pestalotia* (sp.) [13].

In the present work we have chosen thiosemicarbazones with the group 2-ethoxy-3-methoxy-benzaldehyde, which can be considered a ester derivative similar of vanillin, and the fragment *fac*-$[Re(CO)_3]^+$. Besides the interesting bioinorganic properties mentioned above, the exploration of the coordinative behaviour of these ligands against tricarbonylrhenium(I) and the structures resulting of their molecular association and their spectroscopic behaviour, is also worth to be studied.

2. Results and discussion

2.1. Synthesis and spectroscopic characterization

The ligands derived from 2-ethoxy-3-methoxy-benzaldehyde thiosemicarbazone were obtained by refluxing a mixture methanol/water solution for 2 h (Scheme 1).

Reaction of the three ligands with *fac*-$[ReX(CO)_3(CH_3CN)_2]$ afforded six adducts (Scheme 2) with general formula *fac*-$[ReX(CO)_3(HL)]$ (**1**).

Elemental analysis and mass spectrometry confirmed the stoichiometry $[ReX(CO)_3(HL)]$. The mass spectra of the metallic species contains a signal corresponding to the molecular ion, although the peak due to the species $[M-X]^+$ is more intense.

Furthermore, facial geometry around the rhenium atom is suggested by the three strong bands $\nu(C{\equiv}O)$ in IR (sometimes collapsed) in the range 1889–2027 cm^{-1}. The ligand bands corresponding to the N–H groups appear between 3181 and 3508 cm^{-1} and are hardly modified by coordination. Regarding the typical bands from the thiosemicarbazide fragment, the frequencies of the band C=N, in the free ligands in the range 1543–1556 cm^{-1}, shift to the region 1555–1630 cm^{-1} in the spectra of all the complexes. Nevertheless, the band corresponding to the C=S mode shifts from 783 to 788 cm^{-1} in free ligands to 740–771 cm^{-1} in the rhenium complexes, in agreement with the coordination of the ligand by the sulfur atom. This behaviour has been observed in other TSC complexes and it is consistent with the S,N coordination of the ligand [8,11,14,15].

In general, all proton signals in the ^1H NRM spectra in acetone-d_6 of the complexes are shifted at low field (around 0.5 ppm) respect the free ligands. Differently, the signal of the N(2)–H proton moves around 2 ppm. Similar behaviour has been observed in rhenium(I) complexes of hydrazones [16] and thiosemicarbazones [11,14], where the N(2)–H group is a member of the chelate ring resulting after the S,N-coordination. However, when the thiosemicarbazone is coordinated as a S-monodentate ligand, the N(2)–H proton signal behaves as the rest of the ligand signals [10].

To explore the influence of temperature and nature of the rhenium precursor in the reaction product, the reaction of HL^1 with $[ReX(CO)_5]$ were tested in toluene. In the bromine derivative, the

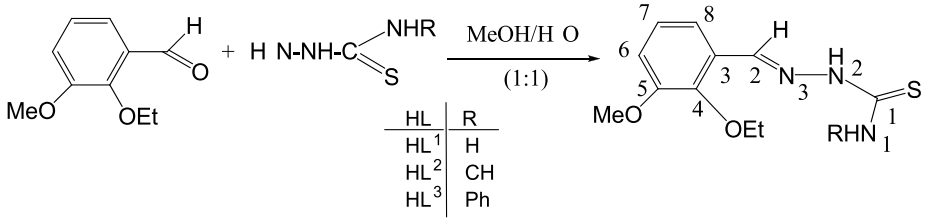

Scheme 1.

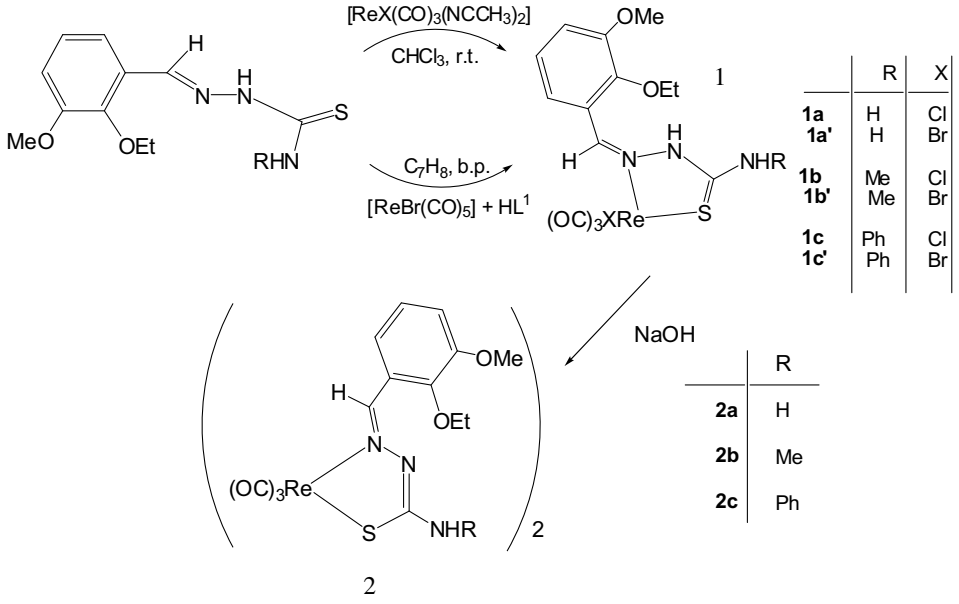

Scheme 2.

characterization of the product showed the formation of the same adduct, $[ReBr(CO)_3(HL^1)]$ (**1a′**), exclusively. However when the chloride derivative was used, the spectroscopic data suggested the coexistence of the compound **1a** and also some product derivate of the deprotonation.

On the other hand, the X-ray study of the crystals obtained from methanol solutions **1b** and **1c** showed the formation of binuclear thiosemicarbazonate complexes (Scheme 2). In a process similar to observed in the rhenium(I) complex of ferrocenylaldehyde thiosemicarbazone [11], the deprotonation of the TSC ligand induces the labilization of the halogen in a position occupied by sulfur atom from other TSC coordinated.

These complexes **2a**, **2b** and **2c** were obtained by reaction of bromine derivatives, **1a′**, **1b′** and **1c′**, with NaOH in methanol. In all of them, the three carbonyl IR bands are consistent with the facial geometry around rhenium atom, and the ν(C=S) bands at 714–740 cm^{-1}, suggest some weakening of the bond. The vibration frequencies of C=N bonds shift to a larger wavenumbers than in free ligands (1610–1710 cm^{-1}).

The ^1H NMR spectra of these compounds in acetone-d_6 show all the proton signals shifted at low field respect to the free ligands and as expected the signals for N(2)–H are absent.

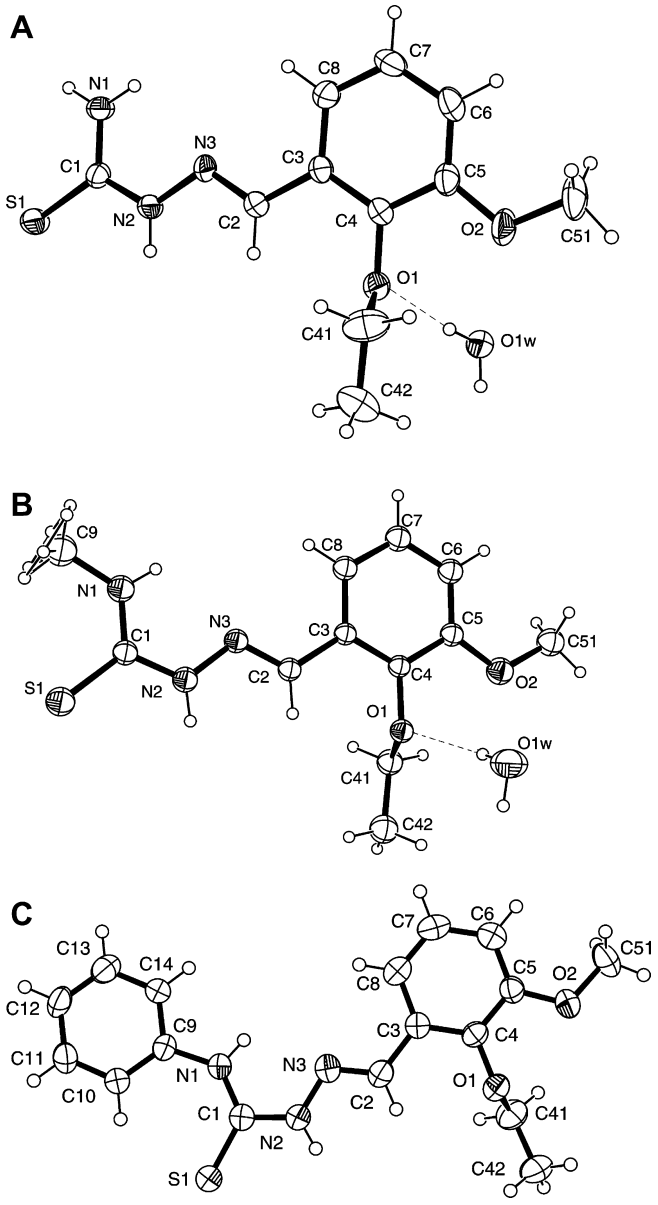

Fig. 1. Molecular structures of $HL^1 \cdot H_2O$ (A), $HL^2 \cdot 1/2H_2O$ (B) and HL^3 (C).

2.2. Crystal and molecular structure of the ligands

The molecular structures of the free ligands are shown in Fig. 1 along with the atomic numbering scheme used. Crystal data and selected bond lengths and angles are listed in Tables 1 and 2, respectively.

Ligands HL^1 and HL^2 crystallized as mono- and hemi-hydrates, respectively, and the water molecule is linked by hydrogen bond to the oxygen atom of the ethoxy group (O(1)W). The role of this molecule in both structures is discussed in detail below. In HL^2, two TCS ligand molecules per asymmetric unit were identified showing differences between distances and angles statistically insignificant and, consequently, the average values are including in Table 2.

In all the cases, the distances C(1)–S(1), C(2)–N(3), N(2)–N(3) and N(2)–C(1) suggest that, in spite of the usual delocalization of π electrons along the thiosemicarbazide chain [17], the canonical form of the free ligand depicted in Scheme 1 is likely the main form in solid state.

The molecular structure of these ligands shows *E* configuration around C(1)–N(2), N(2)–N(3), N(3)–C(2) and C(2)–C(3) bonds. However, *Z* configuration in the C(1)–N(1) bond has been linked with the existence of intramolecular hydrogen-bonding interactions N(1)–H···N(3). The distance N(1)–N(2) decrease from $HL^1 \approx HL^2 > HL^3$ (Table 3). Before conclude that the shortening is due to the increasing of the interaction strength, note that the angle N(1)–C(1)–S(1) widen following the same path. Thus, these findings are also compatible with the increase of steric hindrance of the R group linked to N(1) and the sulfur atom.

In the three cases, the molecule of the ligand can be considered planar: the angles between the ideal plane of the thiosemicarbazide chain N(1)/S(1)/C(1)/N(2)/N(3)/C(2) and the carbon atoms that define the phenyl ring are 7.34(3)°, 6.67(8)° and 2.4(2)° for HL^1, HL^2 and HL^3, respectively.

Table 1
Crystal data, data collection and refinement of the structures of $HL^1 \cdot H_2O$, $HL^2 \cdot 1/2H_2O$ and HL^3

Compound	$HL^1 \cdot H_2O$	$HL^2 \cdot 1/2H_2O$	HL^3
Empirical formula	$C_{11}H_{17}N_3O_3S$	$C_{12}H_{18}N_3O_{2.5}S$	$C_{17}H_{19}N_3O_2S$
Molecular weight	271.34	276.35	329.41
Space group	*C2/c*	$P2_1/n$	*C2/c*
Unit cell dimensions			
a (Å)	20.260(5)	14.893(3)	30.219(6)
b (Å)	7.0868(19)	10.0714(17)	5.6664(11)
c (Å)	20.581(5)	19.671(3)	20.127(4)
β (°)	113.081(5)	101.779(3)	101.714(4)
V (Å^3)	2718.4(12)	2888.4(8)	3374.6(12)
Z	8	8	8
D_{calc} (Mg/m^3)	1.326	1.271	1.297
μ (mm^{-1})	0.243	0.227	0.205
θ Range (°)	2.19–28.04	1.92–28.05	2.07–28.03
Reflections collected	7029	14981	7626
Independent reflections (R_{int})	3010 (0.0863)	6149 (0.0297)	3408 (0.0518)
Maximum/minimum transmission	0.969/0.672	0.930/0.894	0.966/0.865
Goodness-of-fit on F^2	0.775	1.065	0.906
Final R_1/wR_2 indices [$I > 2\sigma(I)$]	0.0548/ 0.0909	0.0444/ 0.1127	0.0648/ 0.1603
R_1/wR_2 indices (all data)	0.1902/ 0.1160	0.0765/ 0.1243	0.1445/ 0.1957

Table 2
Selected bond lengths (Å) and bond angles (°) for $HL^1 \cdot H_2O$, $HL^2 \cdot 1/2H_2O$ and HL^3

	$HL^1 \cdot H_2O$	$HL^2 \cdot 1/2H_2O$[a]	HL^3
S(1)–C(1)	1.691(3)	1.686(11)	1.681(4)
N(1)–C(1)	1.320(3)	1.323(3)	1.329(4)
N(1)–C(9)		1.442(3)	1.414(4)
N(2)–C(1)	1.340(3)	1.352(2)	1.349(4)
N(2)–N(3)	1.376(3)	1.374(2)	1.373(4)
N(3)–C(2)	1.276(3)	1.276(2)	1.275(4)
C(2)–C(3)	1.462(4)	1.464(3)	1.456(5)
N(1)–C(1)–N(2)	117.7(2)	116.8(18)	114.2(3)
N(1)–C(1)–S(1)	122.6(2)	124.2(15)	127.9(3)
N(2)–C(1)–S(1)	119.8(2)	119.0(16)	117.9(3)
C(1)–N(2)–N(3)	119.8(2)	120.1(17)	120.8(3)
C(2)–N(3)–N(2)	114.7(2)	115.8(17)	115.3(3)
N(3)–C(2)–C(3)	120.7(3)	120.9(19)	121.5(3)
C(1)–N(1)–C(9)		124.7(18)	132.9(3)

[a] Average values and standard deviation estimated by the expressions $x = (\sum x_j/\sigma_j^2)/\sum 1/\sigma_j^2$ and $\sigma^2(x) = 1/\sum 1/\sigma_j^2$.

Table 3
Parameters (Å, °) of H-bonding interactions in $HL^1 \cdot H_2O$, $HL^2 \cdot 1/2H_2O$ and HL^3

D–H···A[a]	d(D–H)	d(H···A)	d(D···A)	∠(DHA)
HL1 · H2O				
N(1)–H(1A)···N(3)	0.86	2.29	2.637(3)	104.5
N(1)–H(1A)···O(1W)	0.86	2.22	2.965(3)	145.2
N(2)–H(2)···S(1)#1	0.86	2.54	3.394(3)	171.1
N(1)–H(1B)···O(1W)#2	0.86	2.39	3.136(4)	145.2
O(1W)–H(1W)···S(1)#2	0.83(3)	2.58(4)	3.330(3)	150(3)
O(1W)–H(2W)···O(1)#3	0.91(4)	2.02(4)	2.923(4)	175(4)
HL2 · ½H2O				
N(1A)–H(1A)···N(3A)	0.86	2.23	2.624(2)	107.8
N(1B)–H(1B)···N(3B)	0.86	2.27	2.652(2)	107.3
N(1A)–H(1A)···O(1W)	0.86	2.28	2.988(3)	139.5
N(2A)–H(2AN)···S(1B)	0.86	2.59	3.4365(18)	167.5
N(2B)–H(2BN)···S(1A)	0.86	2.55	3.3900(18)	165.4
O(1W)–H(1W)···O(1A)#4	0.88(3)	2.15(3)	3.009(3)	164(3)
HL3				
N(1)–H(1)···N(3)	0.86	2.13	2.601(3)	113.9
N(2)–H(2)···S(1)#5	0.86	2.64	3.441(3)	154.5

[a] Symmetry transformations used to generate equivalent atoms: #1 = $-x$, y, $-z+½$; #2 = $-x$, $-y+2$, $-z+1$; #3 = $-x-½$, $y+½$, $-z+½$; #4 = $-x$, $-y$, $-z$; #5 = $-x$, $-y-1$, $-z+1$.

The molecular association in $HL^1 \cdot H_2O$ is strongly dominated by the presence of the water molecule. Two HL^1 molecules are associated with two water molecules by N(1)–H···O(1W) interactions (Table 3) showing in both cases the water molecule an acceptor hydrogen behaviour (Fig. 2A). The interaction between a sulfur atom from TSC and the water, which is now a H-bond donor, probably assists to the formation of these "virtual molecular-tetramer". These units are associated by N(2)–H···S(1) interactions along the *c* axis. In turn, these chains are associated by hydrogen bonds between water and the oxygen atoms, O(1), from a neighbouring ethoxy group in the brick-wall-like arrangement showed in Fig. 2B.

As mentioned before, two molecules of HL^2 can be observed per asymmetric unit. Though important differences are not observed in molecular distances and angles, the differences become more marked when the crystal packing is considered. One of the HL^2 molecules is associated with other, crystallographically equivalent (labelled A in Fig. 2C) by two water molecules as in HL^1, involving two hydrogen bonds pairs N(1A)–H···O(1W) and O(1W)–H···O(1A) (Table 3). These molecules are also associated with molecules non-crystallographically equivalent (labelled B) by N(2A)–H···S(1B) and N(2B)–H···S(1A) interactions (Fig. 2C). These units formed by four ligand molecules and two water molecules are packed by weak contacts O(1W)–H···π, in a herringbone pattern as usually observed in aromatic derivatives.

The HL^3 molecules are also coupled N(2)–H···S(1)#5 by hydrogen bond (Fig. 2E) and the dimers are associated in a herringbone pattern by weak interactions involving methoxy and aromatic C–H groups as H-donors and oxygen atom (ethoxy) or π-clouds as acceptors, respectively (Fig. 2F).

2.3. Crystal and molecular structure of $[ReBr(HL^1)(CO)_3] \cdot ½C_7H_8$ (**1a′** · **½C₇H₈**)

Single crystals of the complex **1a′**, obtained from the mother liquor (toluene) contains one solvent molecule per each two molecules of the complex. The toluene molecule is in the cell origin and, consequently, disordered. In the final model we have considered the methyl group on two alternate positions with occupation factors 50% and the aromatic ring centre at the origin. Moreover, two independent molecules that correspond to the two enantiomer of the *fac* configuration (OC-6-33) appear in the asymmetric, although there are also differences concerning the relative orientation of the aromatic ring and the bromo ligand.

The molecular structure of (**1a′** · **½C₇H₈**) together the numbering scheme used is depicted in Fig. 3A. Crystal data and relevant interatomic distances and angles relative to the coordination sphere are included in Tables 4 and 5, respectively.

The ligand HL^1 is coordinated to Re(I) through the sulfur and azomethine nitrogen N(3) atoms. This coordination mode changes the configuration of the bond C(1)–N(2) from *E*, observed in the structure of free ligand HL^1 (*vide supra*), to *Z* to forms a five-membered chelate ring. This ring is approximately planar and the angles respect to the aromatic ring are 39.4(3)° (Re(1) molecule) and 50.3(4)° (Re(2) molecule). The rhenium atom is octahedrally coordinated to three carbonyl carbon atoms in *fac* arrangement, a bromine atom, the azomethine nitrogen and the sulfur atom of the thiosemicarbazone, main distortion being in the angle S–Re–N (<80°) due to the formation of the chelate ring. The bond distances in Re–N(3), Re–S and Re–Br are statistically equivalent in both molecules and they are very similar to observed previously in others *fac*-$Re(CO)_3$ adducts with TSC chelate ligands [8,9,11,14].

Aside the change of the configuration in the bond C(1)–N(2), the coordination of HL^1 to rhenium modifies also the configuration about the C(2)–N(3) bond to *Z*. Both changes and the non-planar structure of the ligand are likely due to steric hindrances between the aromatic ring, and its ether group, with the fragment $\{Re(CO)_3\}$.

Finally, respect to the molecular structure, the non-planar structure of TSC and the metallic fragment asymmetry, allows the coexistence of two possible distributions of 2-ethoxy-3-methoxy-benzaldehyde fragment: one with the group positioned to the direction occupied by the bromine atom and the other in the opposite direction. Both are in the crystal and probably coexist also in solution but, in contrast to ferrocenyl derivatives, they no produce different signals in the ^1H NMR spectrum [11].

The description of the molecular packing in the crystal is complex since the two enantiomers are associated in different fashion. Beside the weak C–H···acceptor interactions, the Re(1) molecule is associated with other symmetrically equivalent molecules (Fig. 3B) by hydrogen bonds between N–H azomethine and thioamide groups and the bromine atom (N(1A)–H(1A1)···Br(1)#1 = 0.86, 2.557, 3.372(8) Å, 158.54; N(2A)–H(2A2)···Br(1) = 0.86, 2.939, 3.465(8) Å, 147.78°; #1 = $-x+2$, $-y+2$, $-z+1$). These associations, and the metric values from these interactions, have been observed in other rhenium(I) thiosemicarbazones derived from ferrocenylcarbaldehyde [11] and β-keto esters [14]. In the present case, the two interactions are reinforced by an additional interaction which involve the thioamide nitrogen and the ethoxy group from the partner molecule.

In addition, the interactions between molecules containing Re(2) atom, involve the bromine atom in a very similar way to

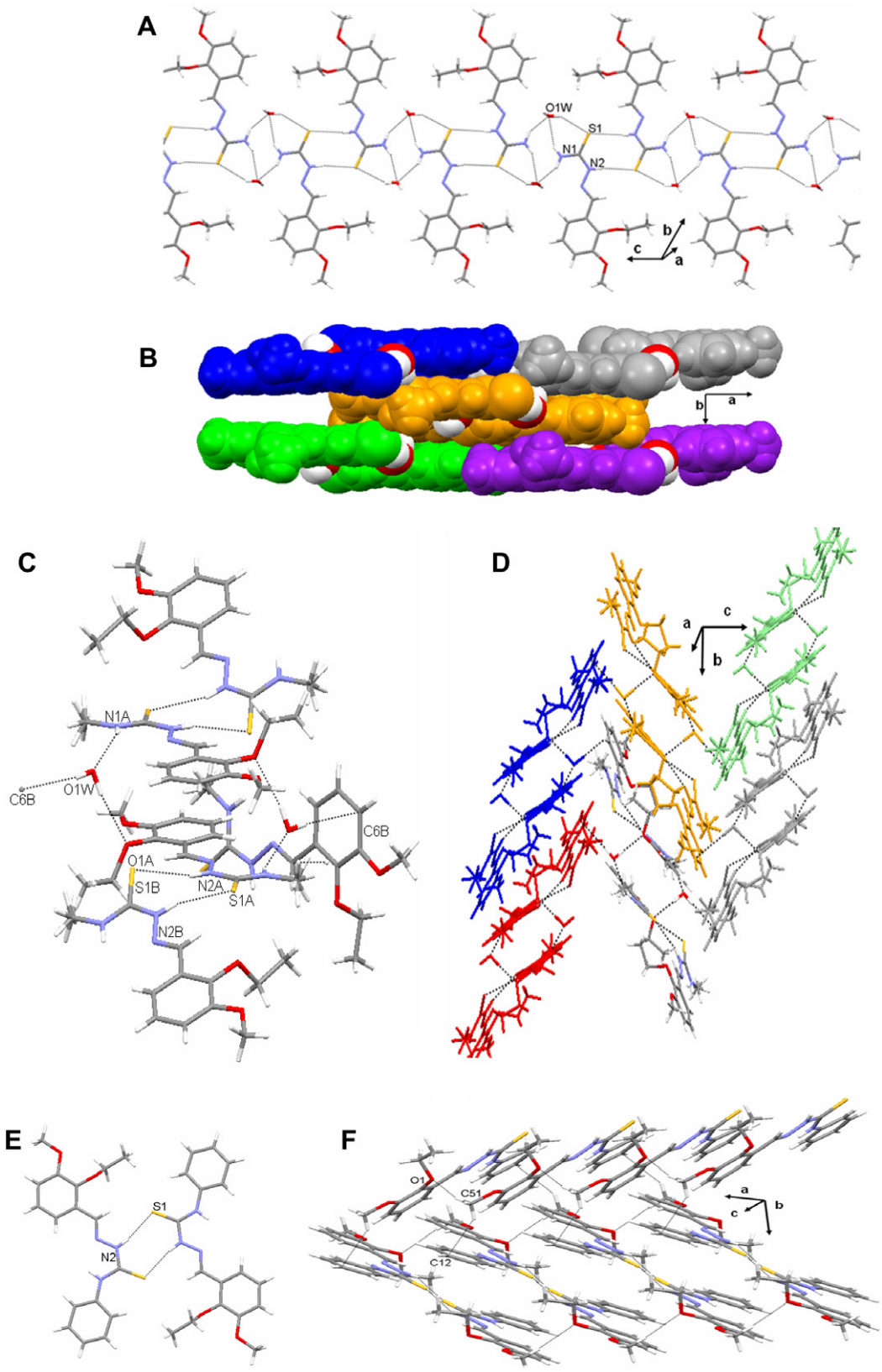

Fig. 2. Supramolecular association in $HL^1 \cdot H_2O$ (A and B), $HL^2 \cdot \frac{1}{2}H_2O$ (C and D) and HL^3 (E and F).

Re(1) molecules, but now, the N(1B)–H group establishes H-bonds (N(1B)–H(1B2)···O(1B)$^{\#2}$ = 0.86, 2.50, 2.934(11) Å, 111.9°; N(1B)–H(1B2)···O(2B)$^{\#2}$ = 0.86, 2.19, 3.042(10) Å, 171.5°; #2 = $-x$, $1-y$, $-z$) with the ether groups of a neighbouring molecule. Consequently, dimers are associated in chains running parallel to *a* axis (Fig. 3C).

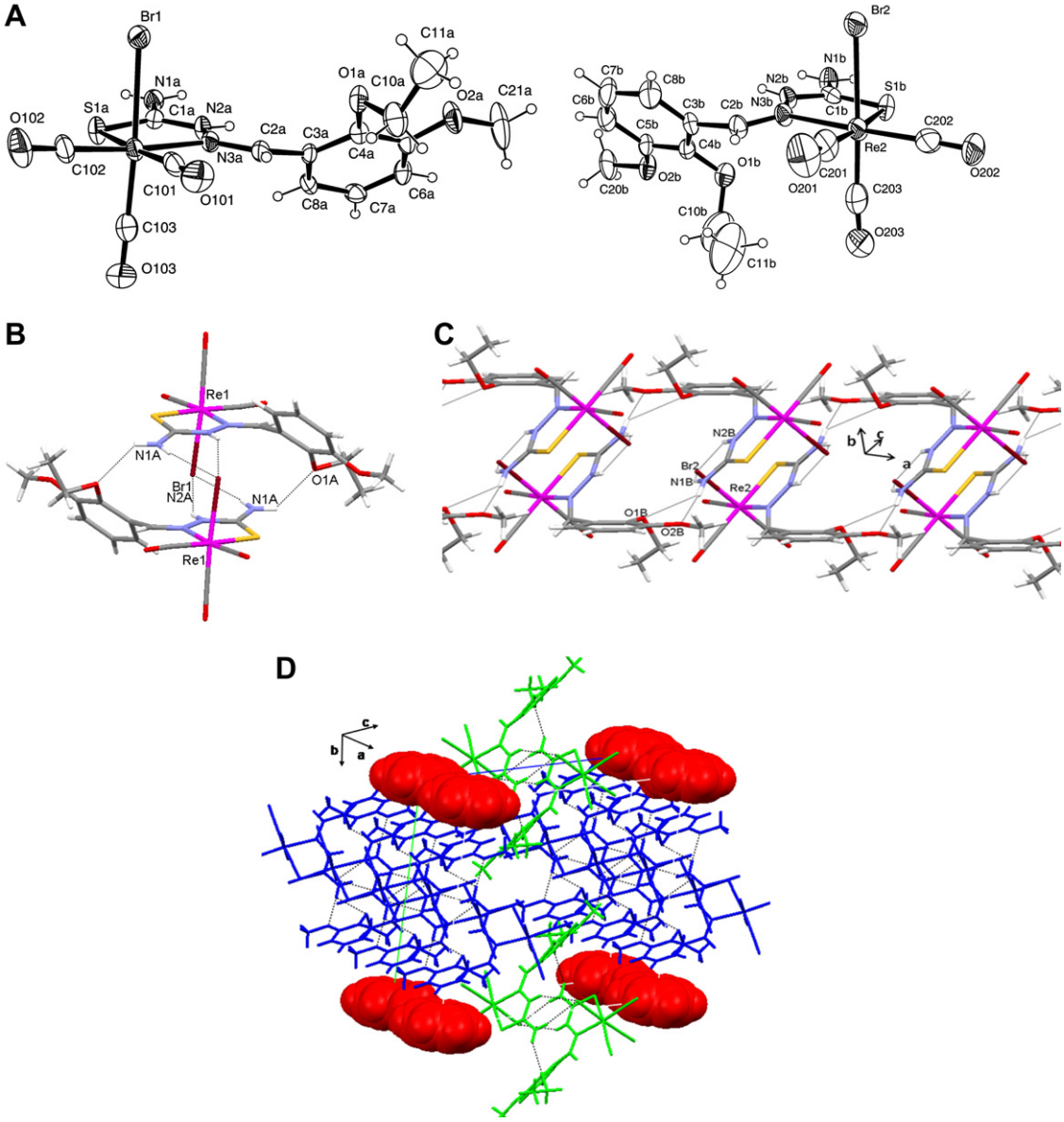

Fig. 3. The molecular structure (A) and crystal packing (B–D) in **1a**′ · **½C$_7$H$_8$**.

Finally, the molecular packing is completed with weak interactions between donor C–H groups and carbonyl as acceptors and can be described considering the packing of the chains of Re(2) molecules, in *b* direction, hosts the Re(1) dimers and toluene molecules (Fig. 3D).

*2.4. Crystal and molecular structure of [Re$_2$(L^2)$_2$(CO)$_6$] (**2b**) and [Re$_2$(L^3)$_2$(CO)$_6$] · 2CH$_3$OH (**2c** · 2CH$_3$OH)*

Single crystals of **2b** and **2c** were obtained by slow concentration from methanol solutions of the previously isolated adducts. The observed disorder of the methyl or the ethoxy group was modulated by refinement of two alternate positions for these groups with occupancies of 80% and 25%. Crystal and structure refinement data for both compounds are showed in Table 4. Relevant length bonds and angles are included in Table 5 meanwhile the molecular structures, showing the numbering scheme used are depicted in Fig. 4.

The ligand deprotonation and the interaction of the rhenium with the sulfur atom of a neighbouring molecule at the position occupied by the halogen atom creates dimers. A difference between both, is that in **2c** this interaction produces centrosymmetric dimers, similar to observed in the ferrocenylcarbaldehyde thiosemicarbazonates [11] but in **2b** both thiosemicarbazonate groups are in the same side of the Re$_2$S$_2$ fragment. This different group orientation and the formation of the Re$_2$S$_2$ diamond, does not impose important differences in bond lengths and angles (Table 6).

The rhenium atoms retains its octahedral coordination, but now interacts with two sulfur atoms, and the sulfur belonging to the partner in the dimer, is farther away than its own sulfur. In fact, the Re–S–Re bridge is relatively asymmetric, as in others dimer structures based on this type of interaction [18,19]. In the diamond Re$_2$S$_2$, the bond angles close to 90° and the distance Re–Re is too long (>3.75 Å) for means any significant bonding interaction.

As observed in ferrocenyl derivatives [11], the Re–N(3) and Re–S(1A) distances are statistically equivalents to the observed in **1a**′. However, the C(1)–S(1) distance is longer than in the free ligands or the adduct **1b**, in agree with a higher thiol character. In addition, the angle between the plane of benzaldehyde ring and the TSC

Table 4
Crystal data and structure refinement of rhenium(I) complexes

Compound	**1a′ · ½C$_7$H$_8$**	**2b**	**2c · 2(CH$_3$OH)**
Empirical formula	$C_{15.5}H_{15}N_3O_5SReBr$	$C_{30}H_{32}N_6O_{10}S_2Re_2$	$C_{40}H_{36}N_6O_{10}S_2Re_2$
Formula weight	623.49	1073.14	1325.44
Space group	$P\bar{1}$	$P2_1/c$	$P\bar{1}$
Unit cell dimensions			
a (Å)	8.0343(9)	10.6586(9)	7.9039(6)
b (Å)	15.5310(17)	16.9065(15)	12.6770(9)
c (Å)	16.9500(18)	21.3813(19)	13.6465(10)
α (°)	93.907(2)		64.4370(10)
β (°)	98.804(2)	91.009(2)	82.0500(10)
γ (°)	96.164(2)		89.9540(10)
V (Å^3)	2070.3(4)	3852.3(6)	1218.99(16)
Z	4	4	1
D_{calc} (Mg/m^3)	2.000	1.850	1.806
μ (mm^{-1})	7.930	6.588	5.177
θ Range (°)	1.88–28.03	1.91–28.03	1.78–28.01
Reflections collected	13435	24785	8019
Independent reflections (R_{int})	9455 (0.0462)	9143 (0.0857)	5596 (0.0223)
Maximum/minimum transmission	0.530/0.357	0.433/0.279	0.541/0.233
Goodness-of-fit on F^2	0.966	0.997	1.097
Final R_1/wR_2 indices [$I > 2\sigma(I)$]	0.0527/0.0945	0.0521/0.1150	0.0264/0.0652
R_1/wR_2 indices (all data)	0.1382/0.1209	0.1371/0.1481	0.0311/0.0781

Table 5
Relevant interatomic distances (Å) and angles (°) for the complex [ReBr(CO)$_3$(HL^1)] · **½C$_7$H$_8$** (**1a′** · **½C$_7$H$_8$**)

Re(1)–C(101)	1.919(12)	Re(2)–C(201)	1.933(16)
Re(1)–C(102)	1.869(12)	Re(2)–C(202)	1.893(13)
Re(1)–C(103)	1.875(13)	Re(2)–C(203)	1.794(18)
Re(1)–N(3A)	2.196(8)	Re(2)–N(3B)	2.204(8)
Re(1)–S(1A)	2.462(3)	Re(2)–S(1B)	2.455(3)
Re(1)–Br(1)	2.6380(12)	Re(2)–Br(2)	2.6452(14)
S(1A)–C(1A)	1.682(10)	S(1B)–C(1B)	1.680(11)
N(1A)–C(1A)	1.318(11)	N(1B)–C(1B)	1.312(12)
C(1A)–N(2A)	1.346(11)	C(1B)–N(2B)	1.350(11)
N(2A)–N(3A)	1.374(10)	N(2B)–N(3B)	1.359(10)
C(102)–Re(1)–C(101)	86.6(5)	C(202)–Re(2)–C(201)	90.0(5)
C(102)–Re(1)–C(103)	89.4(5)	C(203)–Re(2)–C(202)	86.9(6)
C(103)–Re(1)–C(101)	88.9(4)	C(203)–Re(2)–C(201)	89.6(7)
C(102)–Re(1)–N(3A)	174.5(4)	C(202)–Re(2)–N(3B)	174.5(5)
C(103)–Re(1)–N(3A)	95.7(4)	C(203)–Re(2)–N(3B)	93.3(5)
C(101)–Re(1)–N(3A)	95.4(4)	C(201)–Re(2)–N(3B)	95.5(4)
C(102)–Re(1)–S(1A)	98.6(3)	C(202)–Re(2)–S(1B)	95.4(4)
C(103)–Re(1)–S(1A)	92.4(3)	C(203)–Re(2)–S(1B)	92.2(6)
C(101)–Re(1)–S(1A)	174.7(3)	C(201)–Re(2)–S(1B)	174.4(3)
N(3A)–Re(1)–S(1A)	79.3(2)	N(3B)–Re(2)–S(1B)	79.1(2)
C(102)–Re(1)–Br(1)	88.8(3)	C(202)–Re(2)–Br(2)	94.8(4)
C(103)–Re(1)–Br(1)	176.2(3)	C(203)–Re(2)–Br(2)	178.2(4)
C(101)–Re(1)–Br(1)	94.4(3)	C(201)–Re(2)–Br(2)	89.9(5)
N(3A)–Re(1)–Br(1)	85.97(19)	N(3B)–Re(2)–Br(2)	85.0(2)
S(1A)–Re(1)–Br(1)	84.54(8)	S(1B)–Re(2)–Br(2)	88.17(9)
N(2A)–C(1A)–S(1A)	122.7(8)	N(2B)–C(1B)–S(1B)	122.2(8)
C(1A)–N(2A)–N(3A)	121.0(8)	C(1B)–N(2B)–N(3B)	121.7(8)
C(2A)–N(3A)–N(2A)	118.0(8)	C(2B)–N(3B)–N(2B)	117.3(8)

plane (12° and 15° in **2b** and 9.5° in **2c**) shows a more planar ligand in complexes **2b** and **2c** than in **1a′**.

In the supramolecular structure of **2b**, dimers are associated by hydrogen bonds between the N–H thioamide nitrogen group and the oxygen atom of the ethoxy group of a neighbour dimer (N(1A)–H(1A2)···O(1A)$^{\#1}$ = 0.86, 2.268, 2.934(7) Å, 134.32°; #1 = 1 − x, ½ + y, ½ − z). This interaction links the units [Re$_2$(L^2)$_2$(CO)$_6$] in chains running parallel along b axis (Fig. 4C).

In **2c**, the presence of methanol affects the association of the centrosymmetric dimers. The two molecules of methanol are symmetrically independents and they are associated by O(2M)–H···O(1M) bonds and at the same time, one of them establishes a hydrogen chelate bond with two oxygen atoms of the methoxy and ethoxy group (O(1M)–H(1M)···O(2) = 0.82, 2.083, 2.844(8) Å, 154.08°; O(1M)–H(1M)···O(1) = 0.82, 2.592, 3.221(7) Å, 134.56°). The other methanol molecule behaves as hydrogen bond acceptor with the N–H group of a neighbour dimer (N(1)–H(1)···O(2M)$^{\#1}$ = 0.86, 1.976, 2.830(8) Å, 171.65°; #1 = −x, −y, 2 − z). These interactions make ribbons running transverse to the crystallographic directions a and b.

3. Experimental

3.1. Materials and methods

All solvents used for synthesis were dried over appropriate drying agents, degassed using a vacuum line and distilled under an Ar atmosphere [20]. Adducts [ReX(CO)$_3$(CH$_3$CN)$_2$] were synthesized by Farona and Kraus' published methods [21] from the corresponding [ReX(CO)$_5$] [22].

Elemental analyses were carried out on a Fisons EA-1108. Melting points (mp) were determined on a Gallenkamp MFB-595 and are uncorrected. Mass spectra were recorded on a VG Autospec Micromass spectrometer operating under FAB conditions (nitrobenzyl alcohol matrix). Infrared spectra were recorded from KBr pellets on a Bruker Vector 22FT. The ^{1}H NMR spectra were obtained on a Bruker ARX-400 spectrometer from acetone-d_6 solutions.

3.2. General synthesis of the ligands HL^1, HL^2 and HL^3

To a mixture of a water solution (15 mL) of thiosemicarbazide and a methanol solution (15 mL) of 2-ethoxy-3-methoxy-benzaldehyde was added one $H_2SO_{4(c)}$ drop. To avoid the precipitation of 2-ethoxy-3-methoxy-benzaldehyde some methanol (about 15 mL) was added. The reaction mixture was heated under reflux for 2 h. The resulting solid was filtered off and vacuum dried over KOH/CaCl$_2$. Single crystals were obtained after slow evaporation of the mother liquor.

3.2.1. Data for HL^1

Thiosemicarbazide (500 mg, 5.49 mmol)/2-ethoxy-3-methoxybenzaldehyde (0.5 mL, 3.08 mmol). White crystalline solid. Yield: 1783 mg (89.2%). M.p.: 185 °C. *Anal.* Calc. for $C_{11}H_{15}N_3O_2S$: C, 52.1; H, 6.0; N, 16.6; S, 12.6. Found: C, 52.2; H, 6.1; N, 16.4; S, 12.6%. Mass spectrum [m/z (%)]: 254.11(100) [M]$^+$. IR data (KBr, cm^{-1}): 3482m, 3442m, 3282m ν(NH); 1543s ν(C=N); 783w ν(C=S). ^{1}H NMR data (ppm): 10.55s (1) δ(N(2)–H); 8.55s (1) δ(C(2)–H); 7.83s (1) δ(N(1)–H); 7.62m (1) δ(C(7)–H); 7.43s (1) δ(N(1)–H); 7.05s (1) δ(C(6,8)–H); 7.04s (1) δ(C(6,8)–H); 4.06m (2) δ(O(4)–R^2); 3.85s (3) δ(O(5)–R^3); 1.34m (3) δ(O(4)–R^2).

3.2.2. Data for HL^2

4-Methyl-3-thiosemicarbazide (500 mg, 4.75 mmol)/2-ethoxy-3-methoxybenzaldehyde (0.5 mL, 3.08 mmol). Yellow crystalline solid. Yield: 810 mg (81.0%). M.p.: 154 °C. *Anal.* Calc. for $C_{12}H_{17}N_3O_2S$: C, 51.9; H, 6.4; N, 15.7; S, 11.9. Found: C, 51.6; H, 6.8; N, 15.5; S, 11.7%. Mass spectrum [m/z (%)]: 268.09(100) [M]$^+$. IR data (KBr, cm^{-1}): 3508m, 3334m, 3311m ν(NH); 1556s ν(C=N); 788w ν(C=S). ^{1}H NMR data (ppm): 10.49s (1) δ(N(2)–H); 8.52s (1) δ(C(2)–H); 8.26s (1) δ(N(1)–H); 7.57m (1) δ(C(7)–H); 7.05s (1) δ(C(6,8)–H); 7.04s (1) δ(C(6,8)–H); 4.05m (2) δ(O(4)–R^2); 3.84s (3) δ(O(5)–R^3); 3.14d (3) δ(N(1)–R^1); 1.34t (3) δ(O(4)–R^2).

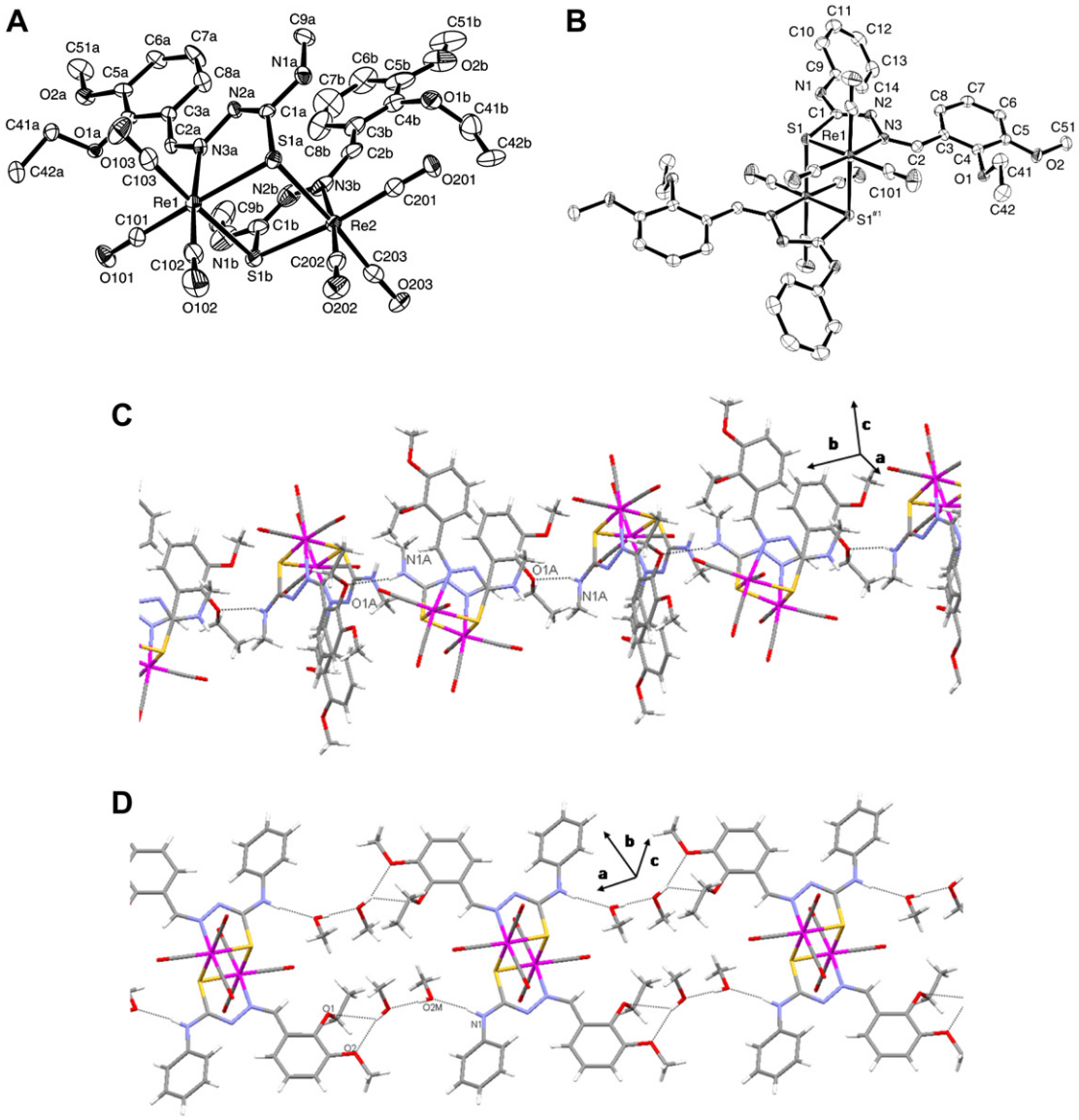

Fig. 4. Molecular structures (hydrogen atoms are omitted for clarity) and the crystal packing in **2b** (A and C) and **2c** · 2(CH_3OH) (B and D).

3.2.3. Data for HL[3]

4-Phenyl-3-thiosemicarbazide (500 mg, 2.99 mmol)/2-ethoxy-3-methoxybenzaldehyde (0.5 mL, 3.08 mmol). White crystalline solid. Yield: 771 mg (77.1%). M.p.: 204 °C. *Anal.* Calc. for $C_{17}H_{19}N_3O_2S$: C, 61.9; H, 5.9; N, 12.7; S, 9.7. Found: C, 61.7; H, 6.0; N, 12.7; S, 9.6%. Mass spectrum [*m*/*z* (%)]: 330.09(100) $[M]^+$. IR data (KBr, cm^{-1}): 3508m, 3333m, 3298m *v*(NH); 1556s *v*(C=N); 788w *v*(C=S). ^1H NMR data (ppm): 10.77s (1) *δ*(N(2)–H); 9.88s (1) *δ*(N(1)–H); 8.64s (1) *δ*(C(2)–H); 7.75d (1) *δ*(C(7)–H); 7.73d (2) *δ*(N(1)–R^1); 7.36t (2) *δ*(N(1)–R^1); 7.19t (1) *δ*(N(1)–R^1); 7.06s (1) *δ*(C(6,8)–H); 7.05s (1) *δ*(C(6,8)–H); 4.10m (2) *δ*(O(4)–R^2); 3.88s (3) *δ*(O(5)–R^3); 1.36m (3) *δ*(O(4)–R^2).

*3.3. General synthesis of the complexes [ReX(CO)$_3$(HL)] (**1**)*

To a solution of the corresponding HL ligand in freshly distilled chloroform (15 mL) was added the corresponding equimolecular quantity of *fac*-[ReX(CO)$_3$(CH_3CN)$_2$] (X = Cl, Br). The yellow mixture was stirred at room temperature for 1 h. The resulting yellow solution was concentrated *in vacuo* to *ca.* 3 mL and stored at room temperature after dropwise addition of diethyl ether until saturation. Yellow solid formed was filtered off and vacuum dried.

*3.3.1. Data for **1a** (HL^1, X = Cl)*

Yield: 227 mg (89.7%). M.p.: 177 °C. *Anal.* Calc. for $C_{14}H_{15}ClN_3O_5SRe$: C, 30.1; H, 2.7; N, 7.5; S, 5.7. Found: C, 29.9; H, 2.6; N, 7.3; S, 5.4%. Mass spectrum [*m*/*z* (%)]: 559 (16.3) $[M]^+$, 524 (100) $[M-Br]^+$, 467 (26.3) $[M-2CO]^+$, 438 (9.7) $[M-3CO]^+$. IR data (KBr, cm^{-1}): 3442m *v*(NH); 2027vs, 1922vs, 1903vs *v*(CO_{fac}); 1630vs *v*(C=N); 757w *v* (C=S). ^1H NMR data (ppm): 12.49s (1) *δ*(N(2)–H); 8.78s (1) *δ*(C(2)–H); 8.20s (2) *δ*(N(1)–H); 7.47d (1) *δ*(C(6)–H); 7.23m (2) *δ*(C(7,8)–H); 4.18m (2) *δ*(O(4)–R^2); 3.89s (3) *δ*(O(5)–R^3); 1.27t (3) *δ*(O(4)–R^2).

*3.3.2. Data for **1a′** (HL^1, X = Br)*

Yield: 240 mg (88.6%). M.p.: 195–202 °C. *Anal.* Calc. for $C_{14}H_{15}BrN_3O_5SRe$: C, 27.8; H, 2.5; N, 6.7; S, 5.3. Found: C, 27.5; H, 2.3; N, 6.1; S, 5.1%. Mass spectrum [*m*/*z* (%)]: 603 (19.7) $[M]^+$, 524 (100) $[M-Br]^+$, 467 (24.3) $[M-2CO]^+$, 438 (10.3) $[M-3CO]^+$. IR data (KBr, cm^{-1}): 3441m, 3420m *v*(NH); 2027vs, 1923vs,

Table 6
Relevant interatomic distances (Å) and angles (°) of $[Re_2(L^2)_2(CO)_6]$ (**2b**) and $[Re_2(L^3)_2(CO)_6] \cdot 2CH_3OH$ (**2c** $\cdot 2CH_3OH$)

	2b	**2c** $\cdot 2(CH_3OH)$
Re(1)–N(3A)/N(3)	2.191(9)	2.202(3)
Re(1)–S(1A)/S(1)	2.458(3)	2.4588(8)
Re(1)–S(1B)/S(1)[a]	2.549(3)	2.5467(9)[a]
Re(1)–C(103)	1.903(14)	1.914(4)
Re(1)–C(101)	1.918(12)	1.917(4)
Re(1)–C(102)	1.936(13)	1.915(4)
Re(2)–N(3B)	2.213(12)	
Re(2)–S(1B)	2.470(3)	
Re(2)–S(1A)	2.557(3)	
Re(2)–C(203)	1.894(14)	
Re(2)–C(202)	1.901(14)	
Re(2)–C(201)	1.921(13)	
S(1A)/S(1)–C(1A)/C(1)	1.780(11)	1.790(3)
C(1A)/C(1)–N(2A)/N(2)	1.276(12)	1.303(5)
N(2A)/N(2)–N(3A)/N(3)	1.384(10)	1.403(3)
C(2A)/C(2)–N(3A)/N(3)	1.285(11)	1.299(5)
S(1B)–C(1B)	1.754(15)	
C(1B)–N(2B)	1.311(16)	
N(2B)–N(3B)	1.281(14)	
C(2B)–N(3B)	1.413(16)	
N(3A)/N(3)–Re(1)–S(1A)/S(1)	79.0(2)	77.19(7)
N(3A)/N(3)–Re(1)–S(1B)/S(1)[a]	90.3(2)	83.56(7)[a]
S(1A)/S(1)–Re(1)–S(1B)/S(1)[a]	82.84(9)	82.02(3) [a]
N(3B)–Re(2)–S(1B)	77.5(4)	
N(3B)–Re(2)–S(1A)	90.9(3)	
S(1B)–Re(2)–S(1A)	82.43(9)	
Re(1)–S(1A)–Re(2)/Re(1)[a]	96.95(9)	97.98(3) [a]
Re(2)–S(1B)–Re(1)	96.88(10)	
C(1A)/C(1)–N(2A)/N(2)–N(3A)/N(3)	117.8(9)	114.0(3)
C(2A)/C(2)–N(3A)/N(3)–N(2A)/N(2)	116.4(9)	116.5(3)
C(1B)–N(2B)–N(3B)	115.2(15)	
C(2B)–N(3B)–N(2B)	110.2(13)	

[a] Equivalents atoms generated by symmetry transformations: $x+1$, $-y+1$, $-z+1$.

1905vs $\nu(CO_{fac})$; 1624s ν(C=N); 757w ν(C=S). ^{1}H NMR data (ppm): 12.53s (1) δ(N(2)–H); 8.72d (1) δ(C(2)–H); 8.19s (2) δ(N(1)–H); 7.37s (1) δ(C(6)–H); 7.21m (2) δ(C(7,8)–H); 4.17m (2) δ(O(4)–R^2); 3.86d (3) δ(O(5)–R^3); 1.23m (3) δ(O(4)–R^2).

This compound was also obtained as **1a**′ $\cdot$ ½C_7H_8 crystals by heating a solution of HL^1 and $[ReBr(CO)_5]$ in toluene for 20 h. Yield: 143 mg (50%).

3.3.3. Data for ***1b*** *(HL^2, X = Cl)*

Yield: 162 mg (72.3%). M.p.: 190–202 °C. *Anal.* Calc. for $C_{15}H_{17}ClN_3O_5SRe$: C, 31.4; H, 3.0; N, 7.3; S, 5.6. Found: C, 31.9; H, 3.2; N, 7.5; S, 5.5%. Mass spectrum [*m*/*z* (%)]: 573 (13.0) $[M]^+$, 538 (100) $[M-Br]^+$, 481 (21.4) $[M-2CO]^+$, 453 (8.8) $[M-3CO]^+$. IR data (KBr, cm^{-1}): 3398m ν(NH); 2023vs, 1899vs $\nu(CO_{fac})$; 1576s ν(C=N); 757w ν(C=S). ^{1}H NMR data (ppm): 12.41s (1) δ(N(2)–H); 8.77s (1) δ(C(2)–H); 8.17s (1) δ(N(1)–H); 7.45d (1) δ(C(6)–H); 7.27d (2) δ(C(7,8)–H); 7.21m (1) δ(C(7,8)–H); 4.18m (2) δ(O(4)–R^2); 3.90d (3) δ(O(5)–R^3); 3.18d (3) δ(N(1)–R^1); 1.27t (3) δ(O(4)–R^2).

3.3.4. Data for ***1b***′ *(HL^2, X = Br)*

Yield: 219 mg (83.6%). M.p.: 219 °C. *Anal.* Calc. for $C_{15}H_{17}BrN_3O_5SRe$: C, 29.2; H, 2.8; N, 6.8; S, 5.2. Found: C, 29.4; H, 2.9; N, 6.7; S, 5.1%. Mass spectrum [*m*/*z* (%)]: 617 (10.0) $[M]^+$, 538 (100) $[M-Br]^+$, 509 (8.6) $[M-CO]^+$, 481 (21.1) $[M-2CO]^+$, 453 (12.6) $[M-3CO]^+$. IR data (KBr, cm^{-1}): 3445m, 3283m ν(NH); 2023vs, 1930vs, 1906vs $\nu(CO_{fac})$; 1596s ν(C=N); 771w ν(C=S). ^{1}H NMR data (ppm): 12.37s (1) δ(N(2)–H); 8.67s (1) δ(C(2)–H); 8.14s (1) δ(N(1)–H); 7.35s (1) δ(C(6)–H); 7.20m (2) δ(C(7,8)–H); 4.16m (2) δ(O(4)–R^2); 3.86d (3) δ(O(5)–R^3); 3.14t (3) δ(N(1)–R^1); 1.23m (3) δ(O(4)–R^2).

3.3.5. Data for ***1c*** *(HL^3, X = Cl)*

Yield: 69 mg (34.8%). M.p.: 214 °C. *Anal.* Calc. for $C_{20}H_{19}ClN_3O_5SRe$: C, 37.7; H, 3.0; N, 6.6; S, 5.0. Found: C, 37.6; H, 3.0; N, 6.6; S, 5.0%. Mass spectrum [*m*/*z* (%)]: 635 (7.4) $[M]^+$, 600 (29.0) $[M-Br]^+$, 543 (7.7) $[M-2CO]^+$. IR data (KBr, cm^{-1}): 3441m ν(NH); 2026vs, 1916vs, 1889vs $\nu(CO_{fac})$; 1555s ν(C=N); 743w ν(C=S). ^{1}H NMR data (acetone-d_6, ppm): 12.56s (1) δ(N(2)–H); 10.24s (1) δ(N(1)–H); 8.91d (1) δ(C(2)–H); 7.48m (5) δ(N(1)–R^1); 7.38m (1) δ(C(6)–H); 7.26m (2) δ(C(7,8)–H); 4.18m (2) δ(O(4)–R^2); 3.90d (3) δ(O(5)–R^3); 1.25t (3) δ(O(4)–R^2).

3.3.6. Data for ***1c***′ *(HL^3, X = Br)*

Yield: 177 mg (76.6%). M.p.: 193 °C. *Anal.* Calc. for $C_{20}H_{19}BrN_3O_5SRe$: C, 35.4; H, 2.8; N, 6.2; S, 4.7. Found: C, 35.6; H, 2.8; N, 6.1; S, 4.9%. Mass spectrum [*m*/*z* (%)]: 679 (11.8) $[M]^+$, 600 (100) $[M-Br]^+$, 571 (10.4) $[M-CO]^+$, 543 (16.3) $[M-2CO]^+$, 514 (14.2) $[M-3CO]^+$. IR data (KBr, cm^{-1}): 3441m ν(NH); 2024vs, 1924vs, 1898vs $\nu(CO_{fac})$; 1565s ν(C=N); 740w ν(C=S). ^{1}H NMR data (ppm): 12.54s (1) δ(N(2)–H); 10.20s (1) δ(N(1)–H); 8.85d (1) δ(C(2)–H); 7.45m (5) δ(N(1)–R^1); 7.35m (1) δ(C(6)–H); 7.24m (2) δ(C(7,8)–H); 4.15m (2) δ(O(4)–R^2); 3.86d (3) δ(O(5)–R^3); 1.21m (3) δ(O(4)–R^2).

3.4. General synthesis of complexes $[Re_2(L)_2(CO)_6]$ (**2**)

To a solution of the corresponding adduct *fac*-$[ReBr(CO)_3(HL)]$ **1,** in 15 mL of dry methanol was added the corresponding equimolar amount of NaOH. The yellow mixture was refluxing for 1 h. The pale yellow solid formed was filtered out and vacuum dried.

3.4.1. Data for ***2a*** *(L^1)*

Yield: 36 mg (21.1%). M.p.: 215–250 °C. *Anal.* Calc. for $C_{28}H_{28}N_6O_{10}S_2Re_2$: C, 30.1; H, 2.7; N, 7.5; S, 5.7. Found: C, 29.9; H, 2.6; N, 7.3; S, 5.4%. Mass spectrum [*m*/*z* (%)]: 1046 (39.5) $[M]^+$. IR data (KBr, cm^{-1}): 3448m, ν(NH); 2021vs, 1908vs $\nu(CO_{fac})$; 1737m ν(C=N); 717w ν(C=S). ^{1}H NMR data (ppm): 9.22s (1) δ(N(1)–H), 8.85s (1) (C(2)–H); 7.78s (1) δ(N(1)–H); 7.65s (1) δ(C(6,8)–H); 7.24s (1) δ(C(6,8)–H); 7.07s δ(C(7)–H); 4.16m (2) δ(O(4)–R^2); 3.88s (3) δ(O(5)–R^3); 1.33t (3) δ(O(4)–R^2).

3.4.2. Data for ***2b*** *(L^2)*

Yield: 64 mg (59.8%). M.p.: 248–253 °C. *Anal.* Calc. for $C_{30}H_{32}N_6O_{10}S_2Re_2$: C, 33.5; H, 3.0; N, 7.8; S, 5.9. Found: C, 33.3; H, 2.8; N, 7.7; S, 5.6%. Mass spectrum [*m*/*z* (%)]: 1074 (9.8) $[M]^+$. IR data (KBr, cm^{-1}): 3443m, 3376m ν(NH); 2028vs, 2015vs, 1917vs, 1895vs $\nu(CO_{fac})$; 1714s ν(C=N); 740w ν(C=S). ^{1}H NMR data (ppm): 8.49s (2) δ(N(1)–H, C(2)–H); 7.63d (1) δ(C(6,8)–H); 7.14d (1) δ(C(6,8)–H); 7.05t δ(C(7)–H); 4.15m (2) δ(O(4)–R^2); 3.87s (3) δ(O(5)–R^3); 2.86s (3) δ(N(1)–R^1); 1.35t (3) δ(O(4)–R^2). Single yellow crystals of **2b** suitable for X-ray diffraction were obtained by slow evaporation of a methanol solution of **1b**.

3.4.3. Data for ***2c*** *(L^3)*

Yield: 21 mg (19.5%). M.p.: >250 °C. *Anal.* Calc. for $C_{40}H_{36}N_6O_{10}S_2Re_2$: C, 40.0; H, 3.0; N, 7.0; S, 5.3. Found: C, 39.9; H, 2.9; N, 6.9; S, 5.1%. Mass spectrum [*m*/*z* (%)]: 1198 (71.4) $[M]^+$. IR data (KBr, cm^{-1}): 3430m ν(NH); 2021vs, 1923vs $\nu(CO_{fac})$; 1707m ν(C=N); 715w ν(C=S). ^{1}H NMR data (ppm): 9.56s (1) δ(N(1)–H); 8.87s (1) δ(C(2)–H); 7.77d (2) δ(C(6,8)–H); 7.46d (1), 7.36t (2), 7.30d (2) δ(N(1)–R^1); 7.09t (1) δ(C(7)–H); 4.24m (1), 4.16m (1) δ(O(4)–R^2); 3.92s (3) δ(O(5)–R^3); 1.32t (3) δ(O(4)–R^2). Yellow single crystals of **2c** $\cdot 2(CH_3OH)$ suitable for X-ray diffraction were obtained by slow evaporation of a methanol solution of **1c**.

3.5. X-ray data collection, structure determination and refinement

Crystallographic data were collected on a Bruker SMART CCD-1000 diffractometer at 293 K using graphite monochromated Mo Kα radiation (λ = 0.71073 Å), and were corrected for Lorentz, polarization and absorption effects [23]. The structures were solved by direct methods using the program SHELX 97 [24]. All non-hydrogen atoms were refined with anisotropic thermal parameters. Hydrogen atoms were inserted at calculated positions and refined as riders [24]. Graphics were produced with PLATON [25] and MERCURY [26].

Acknowledgements

This research was supported by the European Rural Development Found and The Directorates General for Research of Galician Government and Spanish Ministry of Education and Science through projects PGIDIT06PXIB314373PR and CTQ2006-05642/BQU.

Appendix A. Supplementary data

CCDC 683875, 683876, 683877, 683678, 683679 and 683680 contain the supplementary crystallographic data for $HL^1 \cdot H_2O$, $HL^2 \cdot ½H_2O$, $HL^3 \cdot$ **½C$_7$H$_8$**, **2b**, **2c** $\cdot$ 2(CH_3OH). These data can be obtained free of charge via http://www.ccdc.cam.ac.uk/conts/retrieving.html, or from the Cambridge Crystallographic Data Centre, 12 Union Road, Cambridge CB2 1EZ, UK; fax: (+44) 1223-336-033; or e-mail: deposit@ccdc.cam.ac.uk.

References

[1] F. Zobi, B. Spingler, T. Fox, R. Alberto, Inorg. Chem. 42 (2003) 2818.
[2] F. Zobi, O. Blacque, H. Schmalle, B. Spingler, R. Alberto, Inorg. Chem. 43 (2004) 2087.
[3] F. Zobi, B. Spingler, R. Alberto, ChemBioChem 6 (2005) 1397.
[4] K.P. Maresca, J.F. Kronauge, J. Zubieta, J.W. Babich, Inorg. Chem. Commun. 10 (2007) 1409.
[5] M.J.M. Campbell, Coord. Chem. Rev. 15 (1975) 279.
[6] J.S. Casas, M.S. García-Tasende, J. Sordo, Coord. Chem. Rev. 209 (2000) 197.
[7] D.X. West, S.B. Padhye, P.B. Sonawane, Struct. Bond. (Berlin) 76 (1991) 1.
[8] I.G. Santos, U. Abram, R. Alberto, E. Vázquez-López, A. Sánchez, Inorg. Chem. 43 (2004) 1834.
[9] G. Pereiras-Gabián, E.M. Vázquez-López, U. Abram, Z. Anorg. Allg. Chem. 630 (2004) 1665.
[10] R. Carballo, J.S. Casas, E. García-Martínez, G. Pereiras-Gabián, A. Sánchez, U. Abram, E.M. Vázquez-López, CrystEngComm 7 (2005) 113.
[11] R. Carballo, J.S. Casas, E. García-Martínez, G. Pereiras-Gabián, A. Sánchez, J. Sordo, E.M. Vázquez-López, J.C. García-Monteagudo, U. Abram, J. Organomet. Chem. 656 (2002) 1.
[12] A.G. Quiroga, C. Navarro Ranninger, Coord. Chem. Rev. 248 (2004) 119.
[13] K.N. Thimmaiah, G.T. Chandrappa, W.D. Lloyd, C. Párkány, Trans. Met. Chem. (1985) 299.
[14] R. Carballo, J.S. Casas, E. García-Martínez, G. Pereiras-Gabián, A. Sánchez, J. Sordo, E.M. Vázquez-López, Inorg. Chem. 42 (2003) 6395.
[15] G. Pereiras-Gabián, E.M. Vázquez-López, H. Braband, U. Abram, Inorg. Chem. 44 (2005) 834.
[16] P. Barbazán, R. Carballo, U. Abram, G. Pereiras-Gabián, E.M. Vázquez-López, Polyhedron 25 (2006) 3343.
[17] G.J. Palenik, D.F. Rendle, W.S. Carter, Acta Crystallogr., Sect. B 30 (1974) 2390.
[18] G. Thiele, G. Liehr, E. Lindner, Chem. Ber. 107 (1974) 442.
[19] G. Thiele, G. Liehr, E. Lindner, J. Organomet. Chem. 70 (1974) 427.
[20] D.D. Perrin, W.L.F. Armarego, Purification of Laboratory Chemicals, 3rd ed., Oxford, 1988.
[21] M.F. Farona, K.F. Kraus, Inorg. Chem. 9 (1970) 1700.
[22] S.P. Schmidt, W.C. Trogler, F. Basolo, Inorg. Synth. 28 (1990) 160.
[23] G.M. Sheldrick, SADABS, University of Göttingen, Germany, 1996.
[24] G.M. Sheldrick, SHELX-97, Program for the Solution and Refinement of Crystal Structures, v.2, University of Göttingen, Germany, 1997.
[25] A.L. Spek, PLATON, 2002, v. 21.08.03, University of Utrecht, The Netherlands, 2002.
[26] I.J. Bruno, J.C. Cole, P.R. Edgington, M.K. Kessler, C.F. Macrae, P. McCabe, J. Pearson, R. Taylor, Acta Crystallogr., Sect. B 58 (2002) 389.